




GABA decrease is associated with degraded neural specificity in the visual cortex of glaucoma patients

Ji Won Bang ¹✉, Carlos Parra¹, Kevin Yu¹, Gadi Wollstein^{1,2,3}, Joel S. Schuman ^{1,2,3,4} & Kevin C. Chan ^{1,2,3,4,5}✉

Glaucoma is an age-related neurodegenerative disease of the visual system, affecting both the eye and the brain. Yet its underlying metabolic mechanisms and neurobehavioral relevance remain largely unclear. Here, using proton magnetic resonance spectroscopy and functional magnetic resonance imaging, we investigated the GABAergic and glutamatergic systems in the visual cortex of glaucoma patients, as well as neural specificity, which is shaped by GABA and glutamate signals and underlies efficient sensory and cognitive functions. Our study shows that among the older adults, both GABA and glutamate levels decrease with increasing glaucoma severity regardless of age. Further, our study shows that the reduction of GABA but not glutamate predicts the neural specificity. This association is independent of the impairments on the retina structure, age, and the gray matter volume of the visual cortex. Our results suggest that glaucoma-specific decline of GABA undermines neural specificity in the visual cortex and that targeting GABA could improve the neural specificity in glaucoma.

¹Department of Ophthalmology, NYU Grossman School of Medicine, NYU Langone Health, New York University, New York, New York 10017, USA. ²Center for Neural Science, College of Arts and Science, New York University, New York, New York 10003, USA. ³Department of Biomedical Engineering, Tandon School of Engineering, New York University, New York, New York 11201, USA. ⁴Neuroscience Institute, NYU Grossman School of Medicine, NYU Langone Health, New York University, New York, New York 10016, USA. ⁵Department of Radiology, NYU Grossman School of Medicine, NYU Langone Health, New York University, New York, New York 10016, USA. ✉email: JiWon.Bang@nyulangone.org; chuenwing.chan@fulbrightmail.org

Glaucoma is an age-related neurodegenerative disease characterized by the gradual loss of retinal ganglion cells. Such damage disrupts the transmission of the retinal signals to the brain and eventually leads to irreversible blindness. With the increasing aging population, it is estimated that 111.8 million people worldwide will be affected by glaucoma in 2040, suggesting that glaucoma is a major public health problem¹. Nevertheless, the exact mechanisms underlying glaucoma remain unclear. Current clinical treatments focus on intraocular pressure (IOP) reduction with laser, medication, or surgery. However, IOP is a major risk factor but not the cause of the disease. Glaucoma progression in certain patients cannot be attenuated even with controlled IOP, indicating that glaucoma cannot be explained by IOP elevation alone. To reduce the prevalence of this irreversible but preventable disease, we need a better understanding of the mechanisms of glaucoma that will lead to improved treatment strategies beyond IOP control.

An increasing amount of studies has pointed out that glaucomatous degeneration occurs along the visual pathway including the optic nerves^{2,3}, optic chiasm³, lateral geniculate nucleus^{3–9}, optic radiation^{2,10}, and visual cortex^{3,6,7,9,11–13}. Further, recent studies have suggested that glaucoma may share some pathogenic mechanisms with Alzheimer's disease, which is characterized by the accumulation of amyloid β and tau^{14,15}. Critically, glaucoma patients were shown to present abnormal tau proteins in the retina¹⁶ and vitreous fluid¹⁷. Likewise, in animal models of glaucoma, amyloid β and tau were found in the retina¹⁸, lateral geniculate nucleus, and even in the primary visual cortex¹⁹, although the amount of deposits was relatively lower in the visual cortex than in the anterior visual pathway. It suggests that the disease may spread trans-synaptically from the anterior to posterior visual pathways¹⁹.

Accumulation of amyloid β and tau in Alzheimer's disease was found to impair the glutamatergic and GABAergic systems, which are the main excitatory and inhibitory systems in the brain. Exposure to amyloid β can increase extracellular glutamate levels by preventing glutamate uptake^{20,21} or potentiating glutamate release^{22,23}. Elevated amyloid β and tau can also impair synaptic inhibition via downregulation of GABA_A receptor²⁴ and induce substantial loss of GABAergic neurons^{25–27} and GABA-synthetic enzyme²⁵. Of note, loss of GABAergic interneurons co-localizes with tau markers²⁵. If glaucoma patients present amyloid β and tau accumulation in the visual system of the brain, the glutamatergic and/or GABAergic signals are likely to be impaired similar to individuals with Alzheimer's disease.

In particular, the GABAergic signals play a critical role in shaping the response patterns of neuronal populations²⁸. Recent magnetic resonance spectroscopy (MRS) studies revealed a tight relationship between GABAergic signals and neural specificity at the level of neuronal population. As the cortical GABA levels decrease, neural activity patterns associated with different categories become similar, thus more confusable^{29,30}. Increased confusability of neural activity patterns then could potentially degrade behavioral performance³¹. Indeed, loss of neural specificity was observed to be associated with declines in memory performance³² and fluid processing abilities such as executive function and speed of processing³³. Relatedly, glaucoma patients were found to present impairments on some of the perceptual and cognitive functions where GABAergic signals are thought to be involved. These include abnormalities in visual crowding effect³⁴, binocular rivalry^{35–38}, visual categorization^{39,40}, visual attention⁴¹, and cognitive capacity⁴². Further, glaucoma is thought to accelerate the speed of aging process⁴³, which involves gradual reduction of cortical GABA levels^{44–49}. It suggests that glaucomatous degeneration may involve the reduction of GABA to a greater extent than healthy aging and that this reduction of GABA may affect the

neural specificity. Recent hypothesis-independent pathway analysis also implicates GABA and acetyl-CoA metabolism as the novel pathway that is associated with primary open-angle glaucoma⁵⁰. Nevertheless, other than the limited studies on GABAergic involvements in the retina of experimental glaucoma models^{51,52}, no studies have directly examined glaucoma-specific changes in the GABAergic signals and their relationship with neural specificity in the visual cortex of glaucoma patients.

Therefore, in the current study, we investigated whether the GABA and glutamate levels in the visual cortex are affected by glaucoma and whether these neurochemical changes are associated with the neural specificity independent of the impairments of the retina structure and age. To address these questions, we recruited glaucoma patients and age-matched healthy subjects and conducted functional magnetic resonance imaging (fMRI), MRS of the brain, as well as clinical ophthalmic tests including Humphrey visual field perimetry and optical coherence tomography (OCT) of the retina and optic nerve. Using principal component analyses (PCA) and regression modeling, we observed that among our older adult subjects, GABAergic and glutamatergic signals in the visual cortex gradually reduced with increasing severity of glaucoma regardless of age. Further, we observed that the neural specificity in the visual cortex was tightly related to the glaucoma-specific reduction of GABAergic signals, but not that of glutamatergic signals. This association between GABA and neural specificity was observed independent of age or impairments on the retina. These findings indicate the importance of the GABAergic action in the visual cortex and its implications in sensory encoding in glaucoma.

Results

Forty glaucoma patients and twenty-four age-matched healthy subjects underwent clinical ophthalmic exams and magnetic resonance imaging. Their demographic and clinical characteristics can be found in Table 1. Specifically, we obtained each individual's structural and functional images of the whole brain, neurochemical profiles of the visual cortex (Fig. 1) as well as clinical ophthalmic measures including peripapillary retinal nerve fiber layer (pRNFL) thickness, macular ganglion cell-inner plexiform layer (mGCIPL) thickness, optic nerve head cup-to-disc (C/D) ratio, and neuroretinal rim (NRR) area from OCT and the visual field mean deviation (MD) from Humphrey standard automated perimetry.

Glaucoma is accompanied by reduction of GABA in the visual cortex. To examine whether the GABAergic system in the visual cortex alters with disease severity, we first compared the GABA levels across healthy controls, early glaucoma subjects (average MD between eyes better than -6.0 dB) and advanced glaucoma subjects (average MD between eyes worse than -6.0 dB). A one-way ANCOVA while regressing out the effect of age revealed a significant main effect of group ($F(2,54) = 6.666$, $P = 0.003$, partial $\eta^2 = 0.198$; Fig. 2a). Post-hoc tests showed that the levels of GABA are significantly reduced in advanced glaucoma patients compared to healthy controls (early glaucoma vs. healthy controls, Bonferroni-corrected $P = 0.330$, 95% CI = -0.068 to 0.014 , advanced glaucoma vs. healthy controls, Bonferroni-corrected $P = 0.002$, 95% CI = -0.084 to -0.016 , early glaucoma vs. advanced glaucoma, Bonferroni-corrected $P = 0.508$, 95% CI = -0.018 to 0.064).

Next, we also tested whether the impairments on the retina structure, which is a fine-grained, continuous measure of disease severity in the eye are associated with the reduction of GABA levels in the visual cortex. For this, we obtained the marker for retinal structural damage by extracting a common component from each individual's pRNFL thickness, mGCIPL thickness, C/D ratio, and NRR area of left and right eyes using PCA. The PCA

Table 1 Demographic and clinical characteristics of the glaucoma and healthy subjects.

| | Healthy control (n = 24; mean ± S.E.M.) | Early glaucoma (n = 14; mean ± S.E.M.) | Advanced glaucoma (n = 26; mean ± S.E.M.) | Group effect (one-way ANOVA or Chi-squared test) |
|-------------------------------------|--|---|--|--|
| Age (year) | 64.67 ± 1.56 | 65.57 ± 2.40 | 66.19 ± 1.47 | F(2,61) = 0.234, P = 0.792 |
| Sex | 11 M, 13 F | 4 M, 10 F | 13 M, 13 F | $\chi^2(2) = 1.766, P = 0.414$ |
| Average pRNFL thickness (µm) OD | 89.10 ± 2.05 | 72.00 ± 3.24 | 62.04 ± 1.95 | F(2,56) = 40.923, P < 0.001 |
| Average pRNFL thickness (µm) OS | 91.00 ± 1.84 | 76.85 ± 3.02 | 64.62 ± 2.07 | F(2,56) = 40.152, P < 0.001 |
| mGCIPL thickness (µm) OD | 79.06 ± 1.44 | 68.00 ± 3.93 | 59.52 ± 2.10 | F(2,49) = 18.932, P < 0.001 |
| mGCIPL thickness (µm) OS | 78.47 ± 2.00 | 71.75 ± 2.65 | 58.57 ± 1.50 | F(2,49) = 31.705, P < 0.001 |
| NRR area (mm ²) OD | 1.30 ± 0.07 | 0.86 ± 0.09 | 0.64 ± 0.04 | F(2,56) = 34.963, P < 0.001 |
| NRR area (mm ²) OS | 1.35 ± 0.04 | 0.91 ± 0.11 | 0.66 ± 0.04 | F(2,56) = 41.581, P < 0.001 |
| Optic nerve head C/D OD | 0.42 ± 0.04 | 0.70 ± 0.04 | 0.75 ± 0.02 | F(2,56) = 30.195, P < 0.001 |
| Optic nerve head C/D OS | 0.41 ± 0.04 | 0.68 ± 0.03 | 0.75 ± 0.03 | F(2,56) = 35.811, P < 0.001 |
| Visual field mean deviation (dB) OD | -1.65 ± 0.60 | -2.11 ± 0.61 | -17.36 ± 1.65 | F(2,55) = 48.971, P < 0.001 |
| Visual field mean deviation (dB) OS | -1.47 ± 0.40 | -2.54 ± 0.67 | -14.33 ± 1.67 | F(2,55) = 31.239, P < 0.001 |

pRNFL peripapillary retinal nerve fiber layer, mGCIPL macular ganglion cell-inner plexiform layer, NRR neuroretinal rim, C/D cup-to-disc, OD oculus dexter (right eye), OS oculus sinister (left eye).

yielded only one component that had an eigenvalue greater than one, explaining 73.42% of variances of all clinical OCT measures. This component, termed as retinal structure index, was significantly different between groups, with the smallest value in the advanced glaucoma subjects and the greatest value in the healthy controls (main effect of group, $F(2,48) = 85.042, P < 0.001$, partial $\eta^2 = 0.780$; early glaucoma vs. healthy controls, Bonferroni-corrected $P < 0.001$, 95% CI = -1.753 to -0.849, advanced glaucoma vs. healthy controls, Bonferroni-corrected $P < 0.001$, 95% CI = -2.407 to -1.636, early glaucoma vs. advanced glaucoma, Bonferroni-corrected $P < 0.001$, 95% CI = 0.293 to 1.149). Using this component, we ran a linear regression analysis to estimate the GABA levels. The results showed that the retina structure significantly predicted the GABA levels while controlling for age ($T(45) = 2.414, P = 0.020, \beta = 0.337$, partial correlation = 0.339, R^2 change = 0.113; Fig. 2b). It indicates that those who have greater impairments on the retina structure (i.e., lower value of the retinal structure index) present lower amounts of GABA in the visual cortex independent of their ages. The effect of age, however, failed to predict the amount of GABA after controlling for the retinal structure index ($T(45) = 0.596, P = 0.554, \beta = 0.083$, partial correlation = 0.088, R^2 change = 0.007).

Glaucoma is accompanied by reduction of glutamate in the visual cortex. Next, we examined whether the glutamate levels exhibit similar changes as GABA levels in glaucoma. A one-way ANCOVA with a factor of group controlling for age revealed a significant main effect of group ($F(2,56) = 5.157, P = 0.009$, partial $\eta^2 = 0.156$; Fig. 3a). The levels of glutamate were significantly lower in advanced glaucoma patients compared to healthy controls and early glaucoma patients (early glaucoma vs. healthy controls, Bonferroni-corrected $P = 1.000$, 95% CI = -0.110 to 0.153, advanced glaucoma vs. healthy controls, Bonferroni-corrected $P = 0.031$, 95% CI = -0.236 to -0.009, early glaucoma vs. advanced glaucoma, Bonferroni-corrected $P = 0.024$, 95% CI = 0.015 to 0.273). Further, the linear regression analysis demonstrated that the retinal structure index significantly predicted the levels of glutamate while the effect of age was controlled ($T(46) = 2.654, P = 0.011, \beta = 0.358$, partial correlation = 0.364, R^2 change = 0.128; Fig. 3b). It suggests that older adults with greater impairments on the retina structure present lower amounts of glutamate in the visual cortex independent of their ages. Nevertheless, age failed to account for the levels of glutamate when the effect of the retina structure was controlled ($T(46) = -1.525, P = 0.134, \beta = -0.206$, partial correlation = -0.219, R^2 change = 0.042).

Reduction of GABA, but not glutamate predicts deteriorated neural specificity in the visual cortex. Given the significant reduction of GABA and glutamate in the visual cortex of glaucoma patients, we further tested whether the neural specificity is associated with the levels of GABA and glutamate (see Supplementary Fig. 1 for box plots of the neural specificity). For this, we obtained each individual's brain activity patterns across V1, V2, ventral V3, and ventral V4, which overlapped with the MRS voxel. During image acquisition, subjects viewed the horizontal and vertical flickering checkerboards in an alternating order. We measured the marker for neural specificity by calculating the fisher z-transformed correlation coefficient between the brain activation patterns representing horizontal and vertical flickering checkerboards. Here, more negative correlation coefficient value indicated a stronger neural specificity.

To investigate the relationship between neural specificity and the reduced levels of GABA and glutamate, we conducted a series of multiple linear regression analyses while controlling for the effect of age and retinal structure index. Here, we adjusted the effect of the

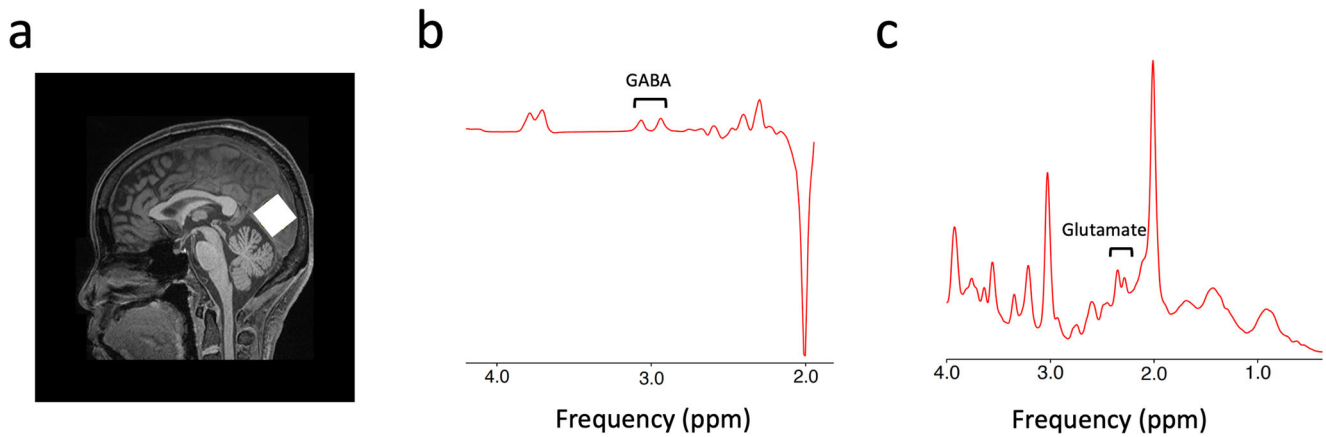


Fig. 1 Sample voxel location for proton MRS and representative spectra for GABA and glutamate. **a** A $2.2 \times 2.2 \times 2.2$ cm³ voxel (white box) was manually positioned along the calcarine sulci on the occipital lobe. **b** A sample spectrum from the MEGA-PRESS sequence for GABA. The GABA peak is at 2.8–3.2 ppm. **c** A sample spectrum from the PRESS sequence for glutamate. The glutamate peak is at 2.2–2.4 ppm.

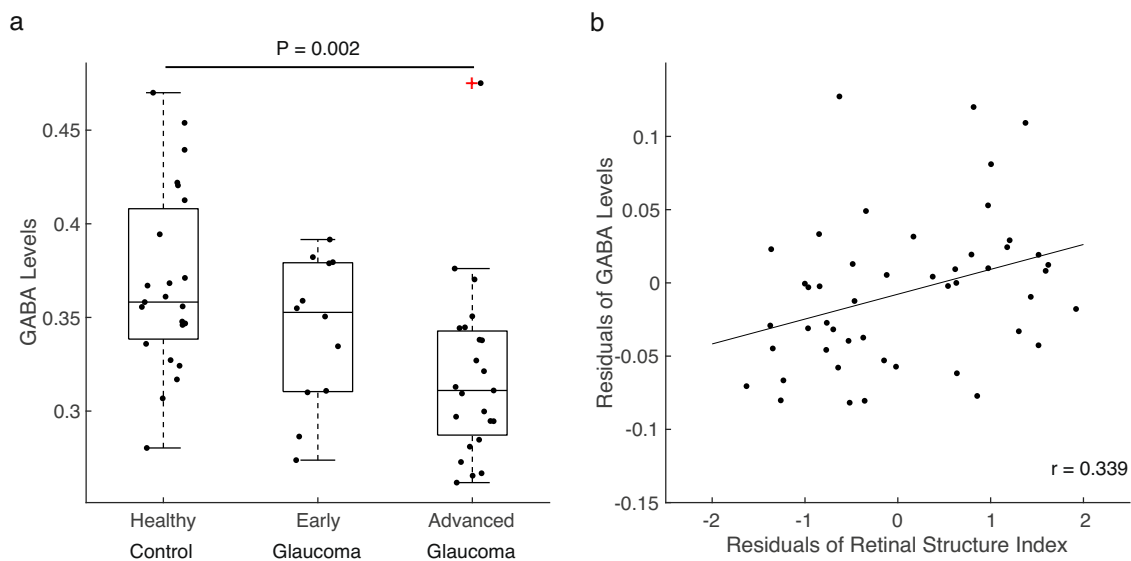


Fig. 2 GABA levels in the visual cortex. **a** The GABA levels (normalized to total creatine levels) were significantly reduced in advanced glaucoma patients compared to healthy controls (Bonferroni-corrected $P = 0.002$). The distributions are represented using box and whisker plots and the outlier is plotted as a red plus sign. In descending order, the lines in the plots represent: maximum, third quartile, median, first quartile, and minimum. Individual data points are overlaid on the box plots. Healthy control: $n = 23$, early glaucoma: $n = 12$, advanced glaucoma: $n = 23$. **b** Individual differences in the retinal structure index were significantly associated with individual differences in the GABA levels after controlling for age ($r = 0.339$, $P = 0.020$; $n = 48$).

retinal structure index in addition to age because the impairments in the retina may block some of the incoming visual signals, resulting in degraded neural specificity. Our regression analyses showed that those with lower GABA levels present weaker neural specificity in the visual cortex when the retinal structure index and age were adjusted ($T(42) = -2.165$, $P = 0.036$, $\beta = -0.317$, partial correlation = -0.317 , R^2 change = 0.088). This association between GABA and neural specificity survived even after we additionally controlled for the levels of glutamate ($T(39) = -2.143$, $P = 0.038$, $\beta = -0.328$, partial correlation = -0.325 , R^2 change = 0.091) and the gray matter volume of the corresponding visual areas ($T(38) = -2.159$, $P = 0.037$, $\beta = -0.334$, partial correlation = -0.331 , R^2 change = 0.094 ; Fig. 4a). In contrast, other factors such as the glutamate levels ($T(38) = 0.439$, $P = 0.663$, $\beta = 0.070$, partial correlation = 0.071 , R^2 change = 0.004 ; Fig. 4b), age ($T(38) = 1.508$, $P = 0.140$, $\beta = 0.223$, partial correlation = 0.238 , R^2 change = 0.046 ; Supplementary Fig. 2a), retinal structure index ($T(38) = -1.690$, $P = 0.099$, $\beta = -0.267$, partial

correlation = -0.264 , R^2 change = 0.057 ; Supplementary Fig. 2b), and the gray matter volume of visual areas ($T(38) = 0.684$, $P = 0.498$, $\beta = 0.100$, partial correlation = 0.110 , R^2 change = 0.009 ; Supplementary Fig. 2c) failed to account for the neural specificity. These results suggest that the most important predictor of neural specificity was the GABA levels in the visual cortex.

In a separate analysis, we conducted a hierarchical regression analysis to test whether the GABA levels explained the significant variance beyond that explained by the retinal structure index, age, glutamate levels, and the gray matter volume of visual areas. The results showed that adding GABA levels to the regression model explained an additional 9.4% of the variations in neural specificity and that this change was significant ($F(1,38) = 4.663$, $P = 0.037$).

After confirming that GABA levels significantly accounted for the neural specificity in the entire sample, we further tested whether the same association could be found within the samples of glaucoma patients and healthy controls separately. In the sample of glaucoma patients, we replicated the results of an association between GABA

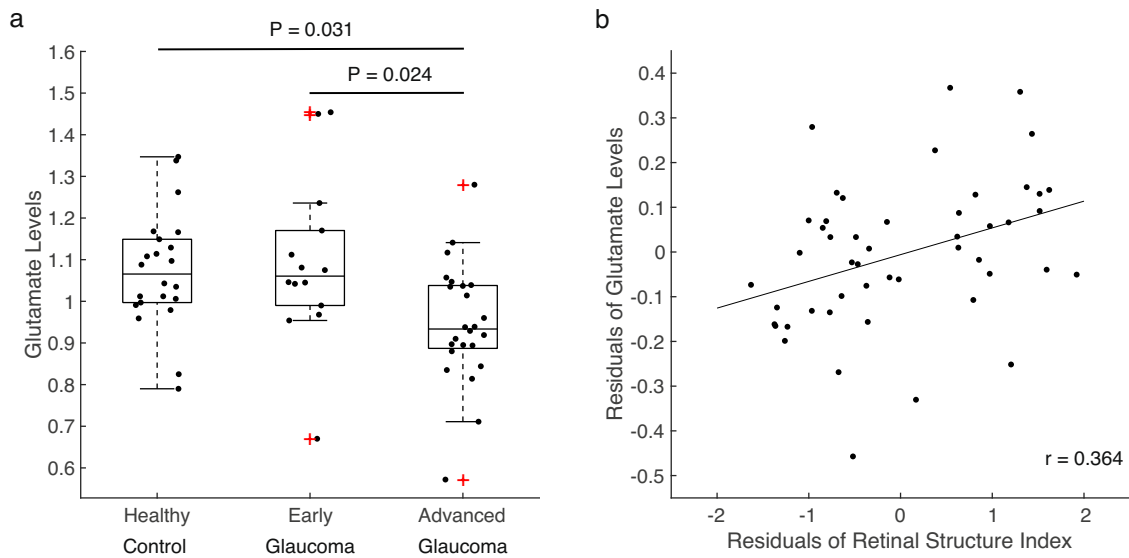


Fig. 3 Glutamate levels in the visual cortex. **a** The glutamate levels (normalized to total creatine levels) were significantly lower in advanced glaucoma patients compared to healthy controls (Bonferroni-corrected $P = 0.031$) and early glaucoma patients (Bonferroni-corrected $P = 0.024$). The distributions are represented using box plots and the outliers are plotted as red plus signs. Individual data points are overlaid on the box plots. Healthy control: $n = 22$, early glaucoma: $n = 14$, advanced glaucoma: $n = 24$. **b** The retinal structure index was positively correlated with the glutamate levels after controlling for age ($r = 0.364$, $P = 0.011$; $n = 49$).

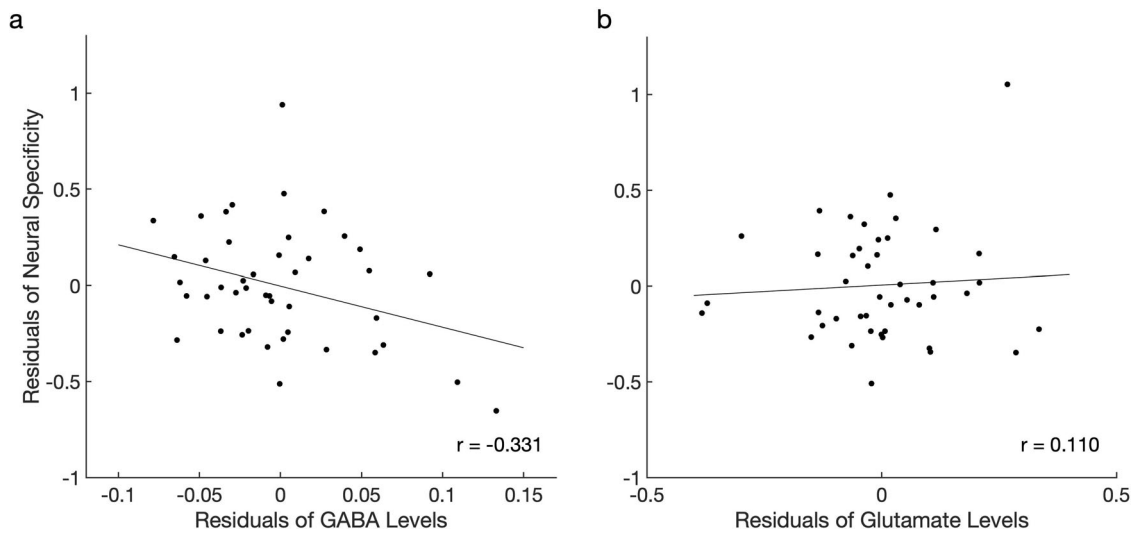


Fig. 4 The relationship between neural specificity, GABA, and glutamate in the visual cortex for the entire sample. **a** The GABA levels were significantly correlated with neural specificity after controlling for the glutamate levels, retinal structure index, age, and the gray matter volume of the visual areas ($r = -0.331$, $P = 0.037$; $n = 44$). **b** The glutamate levels were not associated with neural specificity after adjusting the effects of the GABA levels, retinal structure index, age, and the gray matter volume of the visual areas ($r = 0.110$, $P = 0.498$; $n = 44$).

levels and neural specificity when the retinal structure index and age were controlled ($T(26) = -2.507$, $P = 0.019$, $\beta = -0.410$, partial correlation = -0.416 , R^2 change = 0.166). This association even became stronger when we additionally adjusted the effects of the levels of glutamate ($T(24) = -2.886$, $P = 0.008$, $\beta = -0.517$, partial correlation = -0.508 , R^2 change = 0.219) and the gray matter volume ($T(23) = -2.870$, $P = 0.009$, $\beta = -0.524$, partial correlation = -0.513 , R^2 change = 0.223 ; Fig. 5a). A hierarchical regression analysis also showed that an additional 22.3% of the variations in neural specificity can be explained by adding GABA levels to the regression model ($F(1,23) = 8.235$, $P = 0.009$).

Nevertheless, other factors such as the glutamate levels ($T(23) = 1.635$, $P = 0.116$, $\beta = 0.324$, partial correlation = 0.323 , R^2 change = 0.072 ; Fig. 5b), retina structure index ($T(23) = -1.883$,

$P = 0.072$, $\beta = -0.341$, partial correlation = -0.365 , R^2 change = 0.096 ; Fig. 5c), and the gray matter volume of visual areas ($T(23) = 0.489$, $P = 0.630$, $\beta = 0.085$, partial correlation = 0.101 , R^2 change = 0.006 ; Supplementary Fig. 3) failed to predict the neural specificity. This non-significant effect of the glutamate levels, retina structure index, and the gray matter volume of visual areas in the glaucoma group is consistent with the findings from the entire sample including both glaucoma and healthy subjects.

A discrepancy between the sample of glaucoma patients and the entire sample was seen in the effects of age on neural specificity. Glaucoma patients with older ages presented weaker neural specificity while controlling for other confounding effects including retinal structure index, GABA levels, glutamate levels, and the gray matter volume of the visual areas ($T(23) = 2.610$,

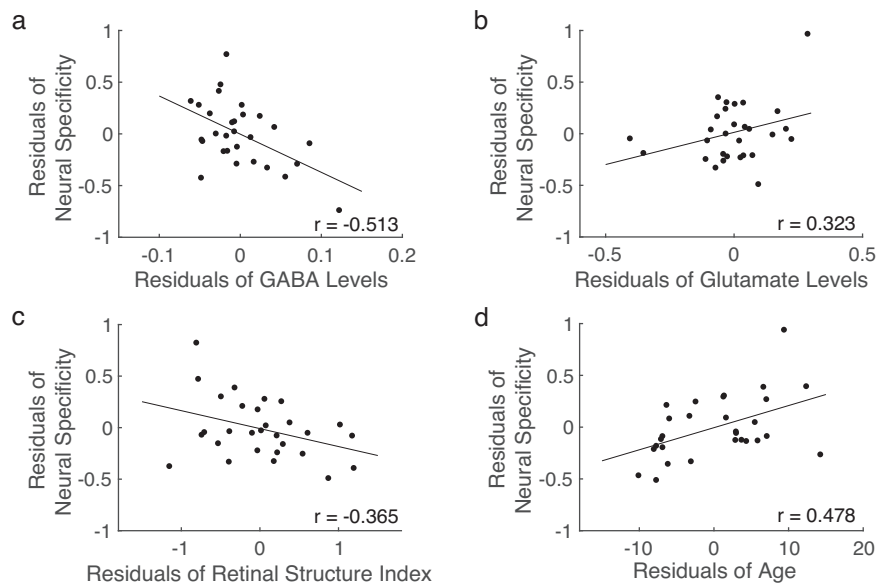


Fig. 5 The relationship between neural specificity, GABA, glutamate, retinal structure index, and age within the glaucoma group. **a** The GABA levels significantly predicted neural specificity after controlling for the glutamate levels, retinal structure index, age, and the gray matter volume ($r = -0.513$, $P = 0.009$; $n = 29$). **b** The glutamate levels were not associated with neural specificity after controlling for the GABA levels, retinal structure index, age, and the gray matter volume ($r = 0.323$, $P = 0.116$; $n = 29$). **c** The retinal structure index was not associated with neural specificity after controlling for the GABA levels, glutamate levels, age, and the gray matter volume ($r = -0.365$, $P = 0.072$; $n = 29$). **d** Age was significantly correlated with neural specificity after adjusting the effects of the GABA levels, glutamate levels, retinal structure index, and the gray matter volume ($r = 0.478$, $P = 0.016$; $n = 29$).

$P = 0.016$, $\beta = 0.496$, partial correlation = 0.478, R^2 change = 0.185; Fig. 5d). This result indicates that age was a meaningful predictor for neural specificity within the sample of glaucoma patients, but not in the entire sample including both glaucoma and healthy subjects.

Finally, we examined whether the same patterns of relationship could be seen within the healthy control group. The results showed that none of GABA, glutamate, age, or retinal structure index was a significant predictor for the neural specificity in healthy controls after adjusting the remaining factors (GABA: $T(9) = -0.594$, $P = 0.567$, $\beta = -0.155$, partial correlation = -0.194 , R^2 change = 0.022; Glutamate: $T(9) = 0.310$, $P = 0.763$, $\beta = 0.087$, partial correlation = 0.103, R^2 change = 0.006; Age: $T(9) = -0.455$, $P = 0.660$, $\beta = -0.119$, partial correlation = -0.150 , R^2 change = 0.013; Retinal structure index: $T(9) = -0.231$, $P = 0.823$, $\beta = -0.060$, partial correlation = -0.077 , R^2 change = 0.003; Supplementary Fig. 4a–d). However, the gray matter volume of visual areas was a significant predictor for the neural specificity in healthy controls ($T(9) = 2.444$, $P = 0.037$, $\beta = 0.659$, partial correlation = 0.632, R^2 change = 0.375; Supplementary Fig. 4e).

Critically, the overall MRS results yielded by using total creatine for normalization were maintained even when we used N-acetyl-aspartate (NAA), another standard reference resonance for normalization. Using NAA for normalization, we still observed a marginal association between the GABA levels and the neural specificity after adjusting the effects of the retinal structure index, age, the levels of glutamate normalized by NAA, and the gray matter volume in the entire sample ($T(38) = -1.890$, $P = 0.066$, $\beta = -0.286$, partial correlation = -0.293 , R^2 change = 0.073). In the sample of glaucoma patients, this association between the GABA level normalized by NAA and the neural specificity became even stronger ($T(23) = -2.659$, $P = 0.014$, $\beta = -0.497$, partial correlation = -0.485 , R^2 change = 0.192).

Discussion

In the current study, we demonstrated that both GABA and glutamate levels in the visual cortex decline with increasing

glaucoma severity. This association between impairments of the retina structure, GABA, and glutamate was independent of age among our older adults. Further, we showed that the reduction of GABA, but not that of glutamate, was associated with the neural specificity in the visual cortex after controlling for confounding effects including age and retinal structural damage. These results provide clear evidence that glaucomatous neurodegeneration involves the reduction of GABA and glutamate levels in the visual cortex and that the reduction of GABA, but not that of glutamate, plays a critical role in degrading neural specificity.

The reduction of GABA levels in the visual cortex of glaucoma patients is consistent with the literature showing that GABA metabolism is a unique pathway associated with glaucoma⁵⁰. Furthermore, GABA is susceptible to the accumulation of amyloid β and tau^{24–27,53}. Prior studies demonstrated that glaucoma involves accumulation of tau in the vitreous fluid¹⁷, retina^{16,18}, lateral geniculate nucleus¹⁹ as well as deposits of amyloid β in the lateral geniculate nucleus and the primary visual cortex¹⁹. Notably, exposure to amyloid β and tau is known to impair the GABAergic systems^{24–27,53}. In animal models of Alzheimer's disease, accumulation of amyloid β led to decreases in the number²⁶ and density of GABAergic neurons before loss of pyramidal cells²⁷. Further, amyloid β was shown to weaken synaptic inhibition via down-regulating GABA_A receptors²⁴. In another animal model expressing high deposits of tau, a substantial decline was observed in the GABA-synthetic enzyme and GABAergic interneurons, which colocalized with tau markers²⁵. This line of studies raises a possibility that glaucoma may share common pathogenic mechanisms with Alzheimer's disease and that accumulation of amyloid β and tau in the visual pathway may promote loss of GABA neurotransmission in glaucoma patients.

In addition to the possible impact of amyloid β and tau on GABA, several other factors may contribute to GABA reduction. First, impaired visual input may facilitate GABA reduction. Visual deprivation was shown to trigger GABA reduction in the primary visual cortex⁵⁴. Given that the visual signals are gradually blocked as glaucoma progresses, it is speculated that its impact on

GABA would increase as well. Consistent with this, our study observed that the GABA levels in the visual cortex measured by MRS decrease with increasing impairments of the retina structure. Second, accelerated aging process in glaucoma may affect GABA levels. Facilitated aging in glaucoma is supported by the finding that glaucoma patients present elevated amount of advanced glycation end products, which are inevitable compounds of the aging process, as well as upregulation of their receptors in the retina and optic nerve head⁴³. Relatedly, the aging process involves impairments of GABAergic systems⁵⁵. In healthy animal models and humans, age-related declines were observed in terms of the number of GABAergic neurons^{56–58}, baseline GABA levels, GABA release, GABA receptor binding⁵⁷, and MRS GABA measures throughout the brain^{44–49}. Therefore, it is possible that the age-related declines of GABA may be accelerated in glaucoma patients. Future studies could address this possibility by obtaining the measures of biological speed of aging from biological assays along with MRS and functional MRI.

In this study, MRS measures of GABA cannot distinguish whether the decreased GABA levels in the visual cortex of glaucoma patients reflect reduction of GABAergic neurons, GABA neurotransmitters, or GABA synthesis⁵⁹. Any combination of these changes could lead to reduced MRS GABA levels. While it is yet unknown which factor contributed the most to our MRS observations, one study using an experimental monkey model observed that after unilateral IOP elevation, the GABA_A receptor protein in the primary visual cortex was reduced¹¹, possibly driven by suppression of visually driven activity⁶⁰. This finding suggests that the declined MRS GABA levels that we observed in the current study are in part reflective of reduced GABA receptor binding. Other possibilities such as reduction of the GABAergic neurons or GABA neurotransmitters need to be further identified in future *in vivo*, *in situ*, and *ex vivo* studies using a finer spatial resolution. Further, it should be noted that in the current study, the GABA-editing technique did not specifically suppress the macromolecules, although macromolecule signals were taken into account in the analysis. Future studies can consider macromolecule-suppressed GABA-edited techniques in order to further reduce the potential contaminations of GABA signals with the macromolecules⁶¹.

The decreased GABA signals in the visual cortex of glaucoma patients suggest that the cortical GABAergic function is likely impaired in glaucoma. GABAergic signals are critical for shaping the response of a single neuron as well as the response patterns of a population of neurons²⁸. At the level of a single neuron, GABA-mediated inhibition can sharpen the neuronal response around the preferred stimulus feature⁶². In line with this, application of GABA agonist increases the neuron's selectivity to preferred stimulus feature, while application of GABA antagonist decreases the neuron's selectivity⁶³. Therefore, it is speculated that the selectivity of neurons in the visual cortex may be undermined in glaucoma patients. At the population level, GABAergic signals are related to the specificity of neuronal activity patterns in response to different stimuli. With lower amount of GABA, neuronal activity patterns become less distinct or more confusable^{29,30}. Consistent with these prior findings, we observed that those who had lower GABA levels displayed less specific neural activity patterns in the visual cortex independent of the age and impairments of the retina structure. It suggests that the declines of GABA and neural specificity in the visual cortex may negatively affect the downstream processes along the lower- to higher-order brain regions^{32,33} in glaucoma.

Alterations of GABA levels and neural specificity in glaucoma patients are likely to have functional influences to various aspects of brain functions. Prior studies showed that GABA levels in healthy subjects are associated with visual-spatial intelligence, visual

surround suppression⁶⁴, motor inhibition⁴⁵, motor learning⁶⁵, general sensorimotor functioning⁴⁹, cognitive performance^{46,48}, experience-dependent plasticity⁶⁶, and sleep⁶⁷. Further, neural specificity was found to be related to memory performance³² and fluid processing ability³³. Therefore, it is reasonable to suspect that these aspects of brain functions may be undermined if the GABA level and the neural specificity are impaired. In line with this speculation, glaucoma patients were found to present abnormalities in perceptual, cognitive functions and sleep quality. Specifically, these abnormalities include elevated visual crowding effect³⁴, impairments on perceptual switch during binocular rivalry^{35–37}, declines in visual categorization^{39,40}, visual attention⁴¹ and cognitive capacity^{39,40,42} as well as sleep disturbance^{68,69}. Thus, we propose that there could be a functional link between GABA reduction and the reported abnormalities in glaucoma patients. Future studies could address this question by employing both MRS and behavioral measures.

In addition to the GABA levels, we observed that the years of age could predict the neural specificity within the sample of glaucoma patients. Specifically, lower neural specificity was associated with older ages. This association is reasonable given that aging is accompanied by degraded neural distinctiveness/discriminability^{29–31,70,71}. However, in the sample of healthy subjects alone, the relationships between GABA, years of age and neural specificity were not observed. This discrepancy could be partly due to the smaller sample size of the healthy controls or could be related to accelerated biological aging process in glaucoma patients. In order to fully understand this discrepancy, we need future studies with a greater sample size.

Another important finding in this study is that the glutamate levels in the visual cortex decline with the impairments on the retinal structure. This observation may appear inconsistent with the literature showing that accumulation of amyloid β leads to increased glutamate levels in the extracellular space^{20,21}. Nevertheless, it should be noted that glutamate and GABA are closely linked to each other in terms of production, function, and reuptake. At the level of production, GABA is synthesized by decarboxylation of glutamate via glutamate acid decarboxylase. At the functional level, the balance between excitation and inhibition is critical for a neuron to function properly. The neurons become dysfunctional when cortical excitation or inhibition is acutely manipulated⁷². Further, increases or decreases in the strength of cortical excitation are naturally accompanied by the corresponding proportional changes in the strength of inhibition^{73,74}. At the level of reuptake, glutamate uptake strengthens inhibitory synapses⁷⁵. Thus, it is possible that reduced glutamate levels in the visual cortex may be at least partially related to the reduced GABA levels. Further, recent studies have demonstrated that amyloid β and glutamatergic signals have multifaceted mechanisms⁷⁶. In the early stage of Alzheimer's disease, glutamatergic activity is elevated leading to hyperexcitability of neurons^{77,78}. However, as Alzheimer's disease progresses, glutamate release and vesicular glutamate transporters become markedly decreased⁷⁹. Prior MRS studies also observed a decreasing pattern of glutamate levels with severity of Alzheimer's disease^{80,81}. Thus, our results of decreased glutamate levels in glaucoma may resemble these progressive glutamate changes in the late phases of Alzheimer's disease.

In the current study, the glutamate levels were not associated with the neural specificity. While it is not clear why the glutamate levels are not linked to the local brain activity, prior studies have consistently shown that the glutamate levels measured during rest are not correlated with the intra-regional brain activity during tasks^{82–87}. Meta-analyses also found evidence in favor of no association between glutamate levels and local brain activity⁸⁸. This is in sharp contrast with the GABA levels which showed largely negative associations with the local brain activity^{82,83,85,89,90}. Up to

date, two explanations have been proposed to interpret the absence of association between glutamate levels and local brain activity. First, the glutamate levels measured during rest may be related to the resting-state brain activity, rather than task-related brain activity⁹¹. Second, glutamatergic neurons detected by MRS may influence the brain activity in distal regions more than the local region through their long-range projections⁸⁸. This interpretation is based on prior studies showing that the glutamate levels are positively correlated with the brain activity outside of the MRS sampling region^{92–94}, but not within the sampling region^{82–87}. However, these explanations remain speculative and thus, need to be further examined in future studies.

While the current study focused on the visual cortex only, it is worth knowing whether the same neurochemical changes occur in the retina of glaucoma patients. A number of patient and experimental animal studies have examined the glutamate-mediated excitotoxicity in the vitreous body and retina in glaucoma^{95–98}. Nevertheless, these studies provided disparate results, making it unclear whether the glutamate in the retina is elevated under glaucoma. Other studies investigating GABA, however, point to a dysfunction of the GABAergic signals in glaucoma. For example, in animal models of glaucoma, the retina showed decreases in the GABA turnover rate, activity of GABA-synthetic enzyme, GABA release and the expression of retinal genes associated with GABAergic systems^{51,99}. Further, studies reported that modulating GABAergic activity in the rat's retina under chronic glaucomatous conditions may improve retinal ganglion cell viability and function^{100,101}. Future studies are warranted to examine whether GABA plays a role in glaucomatous neuroprotection and functional recovery throughout the visual system of the brain.

To conclude, our findings demonstrate a tight link between declines of GABA and neural specificity in the visual cortex of glaucoma patients. Our results suggest that glaucoma-specific declines of GABA undermine neural specificity in the visual cortex and that targeting GABA could improve the neural specificity in glaucoma patients.

Methods

Subjects. The Institutional Review Board of New York University Grossman School of Medicine approved this study. This study adhered to the tenets of the Declaration of Helsinki. Informed consent was obtained from all subjects prior to participation. Forty glaucoma subjects [age = 65.98 ± 1.26 (mean \pm S.E.M.); 42.5% male] and twenty-four healthy controls [age = 64.67 ± 1.56 (mean \pm S.E.M.); 45.8% male] were included in the study between August 2018 and May 2022 at New York University Langone Health's Department of Ophthalmology. All subjects had a best corrected visual acuity (BCVA) of 20/60 or better and showed no past medical history (PMH) or current evidence of retinal or neurological disorders. The demographic and clinical information of those who were included in this study is depicted in Table 1. Subjects in the disease group were clinically diagnosed with primary glaucoma, whereas healthy controls exhibited no clinical evidence of glaucomatous conditions. Subjects were not allowed to participate in the MRI study if they were pregnant or breastfeeding at the time of the study, had any metal parts or fragments in the body with the exception of dental fillings, had conditions such as anxiety or claustrophobia, or had obesity that would hinder placement into the MRI scanner.

Clinical ophthalmic exams. The clinical ophthalmic data for both glaucoma patients and healthy subjects were collected, which included pRNFL thickness, mGCIPL thickness, optic nerve head C/D ratio, and NRR area through an automatic analytic software on board of the Cirrus spectral-domain OCT device (Zeiss, Dublin, CA, USA). Visual field MD was also obtained from the Humphrey Swedish Interactive Thresholding Algorithm (SITA) 24-2 standard (Zeiss, Dublin, CA, USA). The average MD of the left and right eyes combined (OU) were obtained to assign the patients into early or advanced glaucoma group. Early glaucoma was categorized as glaucoma patients with average OU MD better than -6.0 dB and advanced glaucoma was determined as average OU MD worse than -6.0 dB following the previous literature^{102–105}.

MRI data acquisition. Age-matched healthy subjects and glaucoma patients were scanned inside a 3-Tesla MR Prisma scanner (Siemens, Germany) with a 20-channel head coil at the Center for Biomedical Imaging, NYU Langone health, New

York University. For anatomical reconstruction, high-resolution T1-weighted MR images were acquired using a multi-echo magnetization-prepared rapid gradient echo sequence, with 256 slices, voxel size = $0.8 \times 0.8 \times 0.8$ mm, 0-mm slice gap, repetition time (TR) = 2400 ms, echo time (TE) = 2.24 ms, flip angle = 8° , field of view = 256 mm, and bandwidth = 210 Hz per pixel.

For MRS acquisition (see Supplementary Table 1 for details), we manually positioned a $2.2 \times 2.2 \times 2.2$ cm³ voxel along the calcarine sulci in the occipital cortex. The voxel covered parts of the visual cortex including V1, V2, ventral V3, and ventral V4. Shimming was performed by a vendor-provided automated shim tool followed by manual fine adjustment. The shim value defined by the full width at half maximum of the water peak was 13.02 ± 0.13 (mean \pm S.E.M.) for gamma-aminobutyric acid (GABA) and 12.93 ± 0.14 (mean \pm S.E.M.) for glutamate. The concentration of GABA was measured from a voxel using a MESHcher-GARwood-Point RESolved Spectroscopy (MEGA-PRESS) sequence with double-banded pulses, at TR = 1500 ms, TE = 68 ms, number of averages = 172, and scanning duration = 522 s. The final spectrum was obtained by subtracting the 'edit-off' spectrum from 'edit-on' spectrum. The concentration of glutamate was measured from the same voxel using a Point RESolved Spectroscopy (PRESS) sequence, with TR = 3000 ms, TE = 30 ms, number of averages = 99, and scanning duration = 300 s. During both MEGA-PRESS and PRESS scans, subjects performed a fixation task. For two subjects, MRS acquisition could not be completed due to technical issues. Additionally, 30 out of the 64 subjects (15 healthy controls and 15 glaucoma patients) underwent water-unsuppressed PRESS scan with number of averages = 16, and scanning duration = 48 s immediately before the PRESS scan in order to perform water scaling.

After MRS acquisition, functional MR images were acquired using a gradient-echo echo-planar imaging (EPI) sequence, with voxel size = $2.3 \times 2.3 \times 2.3$ mm, TR = 1000 ms, TE = 32.60 ms, and scanning duration = 300 s. During fMRI scan, subjects performed a fixation task while a flickering checkerboard pattern was presented at the horizontal vs. vertical meridians. For four subjects (3 healthy controls and 1 glaucoma patient), fMRI images could not be obtained due to technical issues.

Fixation task. To maintain subjects' attention and vigilance levels across the scans, we provided subjects with the fixation task during MEGA-PRESS and PRESS scans. The fixation point was presented at the center of the gray background and subjects were asked to fixate their eyes at the point. The fixation point changed its color unpredictably from white ([R, G, B] = [255, 255, 255]) to red ([R, G, B] = [255, 127, 127]) and returned to white 1.5 s later. When the button was pressed within a 1.5-s time window, this response was recorded as a hit. If not, the response was recorded as a miss. The mean accuracy (\pm S.E.M.) was $98.87 \pm 0.58\%$. The accuracy did not differ across healthy controls, and early and advanced glaucoma patients ($F(2,32) = 0.263$, $P = 0.770$, partial $\eta^2 = 0.016$).

Neural specificity task. During fMRI scans (1 run=300 s), subjects performed the same fixation task, while the background was filled with flickering checkerboard patterns. The checkerboard patterns were presented at either horizontal or vertical meridians in a gray background. The purpose of adding the flickering checkerboard patterns in the background was to obtain the neural specificity for horizontal and vertical meridians. Each of the horizontal and vertical meridians was presented for 8 s in alternation, with 18 trials for the horizontal meridians and 18 trials for vertical meridians in total. At the first and the last 6-s periods, the fixation point was presented only without any checkerboard patterns. The mean accuracy of the fixation task (\pm S.E.M.) was $94.10 \pm 1.11\%$ and was comparable across healthy controls, and early and advanced glaucoma patients ($F(2,42) = 1.468$, $P = 0.242$, partial $\eta^2 = 0.065$).

MRS data analysis. MRS data was fitted in the frequency domain using the LCModel software¹⁰⁶. We used basis functions that include models of macromolecular spectra to adjust the baseline generated by macromolecular and lipid components. We assessed the quality of fitting by visually inspecting LCModel fitted spectra and examining their Cramer-Rao lower bounds (CRLB) and spectral signal-to-noise (S/N) ratio. Four spectra from the MEGA-PRESS and two spectra from the PRESS scans were excluded from further analyses because of poor fitting (CRLB > 20%, S/N < 8). The CRLB was $8.76 \pm 0.15\%$ (mean \pm S.E.M.) for GABA and $8.65 \pm 0.40\%$ (mean \pm S.E.M.) for glutamate. The S/N ratio was 23.84 ± 0.38 (mean \pm S.E.M.) for GABA and 26.6 ± 1.36 (mean \pm S.E.M.) for glutamate. We normalized the concentrations of GABA and glutamate using the amount of total creatine, which is commonly used as a standard reference resonance^{106,107}. For complementary support, we also normalized the GABA and glutamate concentrations by the amount of N-acetyl-aspartate (NAA). In order to examine whether the concentrations of total creatine and NAA were stable regardless of glaucoma, we also normalized the total creatine and NAA to the water signal using the water-unsuppressed PRESS scans collected from 30 out of the 64 subjects. The absolute values of total creatine and NAA did not differ between groups (total creatine, $F(2,27) = 0.465$, $P = 0.633$, partial $\eta^2 = 0.033$; NAA, $F(2,27) = 1.431$, $P = 0.257$, partial $\eta^2 = 0.096$, one-way ANOVA) and did not have any association with the retina structure index (total creatine, $T(23) = -1.152$, $P = 0.261$, $\beta = -0.234$, $R^2 = 0.055$; NAA, $T(23) = 1.174$, $P = 0.253$, $\beta = 0.238$, $R^2 = 0.056$, linear regression). These findings indicate that the total creatine and NAA were not substantially affected by glaucoma, and can be used as reliable references.

fMRI data analysis. We analyzed fMRI data using Freesurfer software version 7.2 (<http://surfer.nmr.mgh.harvard.edu/>) and MATLAB. The fMRI data was pre-processed with motion correction but not with spatial or temporal smoothing. Then the functional data was registered to the individual's structural template. We extracted the blood-oxygenation-level-dependent (BOLD) signals from the individual's region-of-interest (ROI) masks generated from Freesurfer's cortical reconstruction process. The ROI masks that we used were four cytoarchitectonic areas in the occipital lobe (hOc1-hOc4v) which spatially overlapped with the location of the MRS voxel. The extracted BOLD signals were then shifted by 6 s to account for the hemodynamic delay. We excluded voxels with spikes greater than 10 standard deviations from the mean and removed the linear trend in the BOLD time course. Then we normalized the BOLD signals using z-score for each voxel. All volumes were included in the analysis.

Calculation of neural specificity. We defined the neural specificity as the dissimilarity in brain responses between different visual conditions. For this, we averaged the z-normalized BOLD signals of each voxel across 8 volumes (8 s) which corresponded to the duration of horizontal/vertical meridian presentation. These BOLD signals of each voxel were then averaged across 18 trials of horizontal meridians or 18 trials of vertical meridians separately. Given that these two patterns of BOLD signals represented the horizontal or vertical meridians, we computed the Fisher z-transformed correlation coefficient between these two representations to obtain multi-voxel pattern similarity. Finally, we averaged the correlation coefficients across V1, V2, ventral V3, and ventral V4.

Statistics and reproducibility. The sample size was not predetermined but similar or even greater to those reported in prior studies^{2,3,10,12,13,108}. The investigators were not blinded to disease diagnosis during data collection. For all statistical comparisons, we conducted two-tailed parametric tests with $P < 0.05$ as the criterion for statistical significance. For ANOVAs, we assessed the assumption of homogeneity of variances using Levene's test. The following post-hoc tests were conducted with Bonferroni corrections. For multiple regression analyses, we confirmed that the assumptions of independence of observations and non-multicollinearity were not violated using the Durbin-Watson statistic and tolerance/VIF values. Further, we extracted a common component from clinical ophthalmic measures including pRNFL thickness, mGCIPL thickness, optic nerve head C/D ratio, and NRR area for each individual using PCA. Then we entered this component, a measure of retina structure in the regression model rather than entering all clinical ophthalmic measures because the clinical measures were highly correlated to each other, violating the non-multicollinearity. We set the criteria of selecting the component in the PCA as the eigenvalue higher than one. To verify that the overall MRS results hold regardless of the method of normalization, we used NAA in addition to total creatine for normalization.

Apparatus. We created all visual stimuli in MATLAB using Psychophysics Toolbox³¹⁰⁹. The stimuli were presented via an MRI-compatible projector (1024 × 768 resolution, 60 Hz refresh rate).

Inclusion and ethics statement. The authors followed the recommendations set out in the Global Code of Conduct for Research in Resource-Poor Settings. The research was determined and conducted by local researchers. The roles and responsibilities were agreed amongst collaborators ahead of the research. This research did not involve any of the health, safety, security or other risk to researchers, and did not have any severe restrictions in the setting of the researchers. This study did not result in any of the stigmatization, incrimination, discrimination or personal risk. The authors took local and regional research relevant to the current study into account in citations.

Reporting summary. Further information on research design is available in the Nature Portfolio Reporting Summary linked to this article.

Data availability

All data underlying the results and figures are freely available in OSF with the identifier doi: 10.17605/OSF.IO/85CDS (<https://osf.io/85cds/>)¹¹⁰

Code availability

All statistical codes for SPM are freely available in OSF with the identifier doi: 10.17605/OSF.IO/85CDS (<https://osf.io/85cds/>)¹¹⁰

Received: 23 November 2022; Accepted: 5 May 2023;

Published online: 29 June 2023

References

1. Tham, Y. C. et al. Global prevalence of glaucoma and projections of glaucoma burden through 2040: a systematic review and meta-analysis. *Ophthalmology* **121**, 2081–2090 (2014).
2. Garaci, F. G. et al. Optic nerve and optic radiation neurodegeneration in patients with glaucoma: in vivo analysis with 3-T diffusion-tensor MR imaging. *Radiology* **252**, 496–501 (2009).
3. Zikou, A. K. et al. Voxel-based morphometry and diffusion tensor imaging of the optic pathway in primary open-angle glaucoma: a preliminary study. *AJNR Am. J. Neuroradiol.* **33**, 128–134 (2012).
4. Weber, A. J., Chen, H., Hubbard, W. C. & Kaufman, P. L. Experimental glaucoma and cell size, density, and number in the primate lateral geniculate nucleus. *Invest Ophthalmol. Vis. Sci.* **41**, 1370–1379 (2000).
5. Yucel, Y. H., Zhang, Q., Gupta, N., Kaufman, P. L. & Weinreb, R. N. Loss of neurons in magnocellular and parvocellular layers of the lateral geniculate nucleus in glaucoma. *Arch. Ophthalmol.* **118**, 378–384 (2000).
6. Crawford, M. L., Harwerth, R. S., Smith, E. L. 3rd, Shen, F. & Carter-Dawson, L. Glaucoma in primates: cytochrome oxidase reactivity in parvo- and magnocellular pathways. *Invest Ophthalmol. Vis. Sci.* **41**, 1791–1802 (2000).
7. Imamura, K. et al. Molecular imaging reveals unique degenerative changes in experimental glaucoma. *Neuroreport* **20**, 139–144 (2009).
8. Chaturvedi, N., Hedley-Whyte, E. T. & Dreyer, E. B. Lateral geniculate nucleus in glaucoma. *Am. J. Ophthalmol.* **116**, 182–188 (1993).
9. Gupta, N., Ang, L. C., Noel de Tilly, L., Bidaise, L. & Yucel, Y. H. Human glaucoma and neural degeneration in intracranial optic nerve, lateral geniculate nucleus, and visual cortex. *Br. J. Ophthalmol.* **90**, 674–678 (2006).
10. Engelhorn, T. et al. Diffusion tensor imaging detects rarefaction of optic radiation in glaucoma patients. *Acad. Radio.* **18**, 764–769 (2011).
11. Lam, D. Y., Kaufman, P. L., Gabelt, B. T., To, E. C. & Matsubara, J. A. Neurochemical correlates of cortical plasticity after unilateral elevated intraocular pressure in a primate model of glaucoma. *Invest. Ophthalmol. Vis. Sci.* **44**, 2573–2581 (2003).
12. Boucard, C. C. et al. Changes in cortical grey matter density associated with long-standing retinal visual field defects. *Brain* **132**, 1898–1906 (2009).
13. Murphy, M. C. et al. Retinal Structures and Visual Cortex Activity are Impaired Prior to Clinical Vision Loss in Glaucoma. *Sci. Rep.* **6**, 31464 (2016).
14. Ghiso, J. A., Doudevski, I., Ritch, R. & Rostagno, A. A. Alzheimer's disease and glaucoma: mechanistic similarities and differences. *J. Glaucoma* **22**, S36–S38 (2013).
15. Sen, S., Saxena, R., Tripathi, M., Vibha, D. & Dhiman, R. Neurodegeneration in Alzheimer's disease and glaucoma: overlaps and missing links. *Eye (Lond.)* **34**, 1546–1553 (2020).
16. Gupta, N., Fong, J., Ang, L. C. & Yucel, Y. H. Retinal tau pathology in human glaucomas. *Can. J. Ophthalmol.* **43**, 53–60 (2008).
17. Yoneda, S. et al. Vitreous fluid levels of beta-amyloid(1-42) and tau in patients with retinal diseases. *Jpn. J. Ophthalmol.* **49**, 106–108 (2005).
18. Chiasseu, M. et al. Tau accumulation, altered phosphorylation, and missorting promote neurodegeneration in glaucoma. *J. Neurosci.* **36**, 5785–5798 (2016).
19. Yan, Z. et al. Elevated intraocular pressure induces amyloid-beta deposition and tauopathy in the lateral geniculate nucleus in a monkey model of glaucoma. *Invest. Ophthalmol. Vis. Sci.* **58**, 5434–5443 (2017).
20. Fernandez-Tome, P., Brera, B., Arevalo, M. A. & de Ceballos, M. L. Beta-amyloid25-35 inhibits glutamate uptake in cultured neurons and astrocytes: modulation of uptake as a survival mechanism. *Neurobiol. Dis.* **15**, 580–589 (2004).
21. Harris, M. E. et al. Amyloid beta peptide (25-35) inhibits Na⁺-dependent glutamate uptake in rat hippocampal astrocyte cultures. *J. Neurochem.* **67**, 277–286 (1996).
22. Chin, J. H., Ma, L., MacTavish, D. & Jhamandas, J. H. Amyloid beta protein modulates glutamate-mediated neurotransmission in the rat basal forebrain: involvement of presynaptic neuronal nicotinic acetylcholine and metabotropic glutamate receptors. *J. Neurosci.* **27**, 9262–9269 (2007).
23. Kabogo, D., Rauw, G., Amritraj, A., Baker, G. & Kar, S. ss-amyloid-related peptides potentiate K⁺-evoked glutamate release from adult rat hippocampal slices. *Neurobiol. Aging* **31**, 1164–1172 (2010).
24. Ulrich, D. Amyloid-beta impairs synaptic inhibition via GABA(A) Receptor Endocytosis. *J. Neurosci.* **35**, 9205–9210 (2015).
25. Levenson, J. et al. Tau pathology induces loss of GABAergic interneurons leading to altered synaptic plasticity and behavioral impairments. *Acta Neuropathol. Commun.* **1**, 34 (2013).
26. Krantic, S. et al. Hippocampal GABAergic neurons are susceptible to amyloid-beta toxicity in vitro and are decreased in number in the Alzheimer's disease TgCRND8 mouse model. *J. Alzheimers Dis.* **29**, 293–308 (2012).
27. Ramos, B. et al. Early neuropathology of somatostatin/NPY GABAergic cells in the hippocampus of a PS1xAPP transgenic model of Alzheimer's disease. *Neurobiol. Aging* **27**, 1658–1672 (2006).
28. Isaacson, J. S. & Scanziani, M. How inhibition shapes cortical activity. *Neuron* **72**, 231–243 (2011).

29. Chamberlain, J. D. et al. GABA levels in ventral visual cortex decline with age and are associated with neural distinctiveness. *Neurobiol. Aging* **102**, 170–177 (2021).
30. Lalwani, P. et al. Neural distinctiveness declines with age in auditory cortex and is associated with auditory GABA levels. *Neuroimage* **201**, 116033 (2019).
31. Simmonite, M. & Polk, T. A. Age-related declines in neural distinctiveness correlate across brain areas and result from both decreased reliability and increased confusability. *Neuropsychol. Dev. Cogn. B: Aging Neuropsychol. Cogn.* **29**, 483–499 (2022).
32. Fandakova, Y., Leckey, S., Driver, C. C., Bunge, S. A. & Ghetti, S. Neural specificity of scene representations is related to memory performance in childhood. *Neuroimage* **199**, 105–113 (2019).
33. Park, J., Carp, J., Hebrank, A., Park, D. C. & Polk, T. A. Neural specificity predicts fluid processing ability in older adults. *J. Neurosci.* **30**, 9253–9259 (2010).
34. Ogata, N. G. et al. Visual crowding in glaucoma. *Invest. Ophthalmol. Vis. Sci.* **60**, 538–543 (2019).
35. Tarita-Nistor, L., Samet, S., Trope, G. E. & Gonzalez, E. G. Intra- and inter-hemispheric processing during binocular rivalry in mild glaucoma. *PLoS ONE* **15**, e0229168 (2020).
36. Issashar Leibovitch, G., Trope, G. E., Buys, Y. M. & Tarita-Nistor, L. Perceptual grouping during binocular rivalry in mild glaucoma. *Front Aging Neurosci.* **14**, 833150 (2022).
37. Joao, C. A. R., Scanferla, L. & Jansonius, N. M. Binocular interactions in glaucoma patients with nonoverlapping visual field defects: contrast summation, rivalry, and phase combination. *Invest. Ophthalmol. Vis. Sci.* **62**, 9 (2021).
38. Tarita-Nistor, L., Samet, S., Trope, G. E. & Gonzalez, E. G. Dominance wave propagation during binocular rivalry in mild glaucoma. *Vis. Res.* **165**, 64–71 (2019).
39. Lenoble, Q., Lek, J. J. & McKendrick, A. M. Visual object categorisation in people with glaucoma. *Br. J. Ophthalmol.* **100**, 1585–1590 (2016).
40. Roux-Sibilon, A. et al. Scene and human face recognition in the central vision of patients with glaucoma. *PLoS ONE* **13**, e0193465 (2018).
41. Swenor, B. K. et al. Impact of the ability to divide attention on reading performance in glaucoma. *Invest. Ophthalmol. Vis. Sci.* **58**, 2456–2462 (2017).
42. Gangeddu, V., Ranchet, M., Akinwuntan, A. E., Bollinger, K. & Devos, H. Effect of cognitive demand on functional visual field performance in senior drivers with glaucoma. *Front. Aging Neurosci.* **9**, 286 (2017).
43. Tezel, G., Luo, C. & Yang, X. Accelerated aging in glaucoma: immunohistochemical assessment of advanced glycation end products in the human retina and optic nerve head. *Invest. Ophthalmol. Vis. Sci.* **48**, 1201–1211 (2007).
44. Chalavi, S. et al. The neurochemical basis of the contextual interference effect. *Neurobiol. Aging* **66**, 85–96 (2018).
45. Hermans, L. et al. Brain GABA levels are associated with inhibitory control deficits in older adults. *J. Neurosci.* **38**, 7844–7851 (2018).
46. Simmonite, M. et al. Age-related declines in occipital GABA are associated with reduced fluid processing ability. *Acad. Radio.* **26**, 1053–1061 (2019).
47. Gao, F. et al. Edited magnetic resonance spectroscopy detects an age-related decline in brain GABA levels. *Neuroimage* **78**, 75–82 (2013).
48. Porges, E. C. et al. Frontal gamma-aminobutyric acid concentrations are associated with cognitive performance in older adults. *Biol. Psychiatry Cogn. Neurosci. Neuroimaging* **2**, 38–44 (2017).
49. Cassidy, K. et al. Sensorimotor network segregation declines with age and is linked to GABA and to sensorimotor performance. *Neuroimage* **186**, 234–244 (2019).
50. Bailey, J. N. et al. Hypothesis-independent pathway analysis implicates GABA and acetyl-CoA metabolism in primary open-angle glaucoma and normal-pressure glaucoma. *Hum. Genet.* **133**, 1319–1330 (2014).
51. Moreno, M. C. et al. Effect of ocular hypertension on retinal GABAergic activity. *Neurochem. Int.* **52**, 675–682 (2008).
52. Zhou, X. et al. Differential modulation of GABAA and NMDA receptors by an alpha7-nicotinic acetylcholine receptor agonist in chronic glaucoma. *Front. Mol. Neurosci.* **10**, 422 (2017).
53. Najm, R., Jones, E. A. & Huang, Y. Apolipoprotein E4, inhibitory network dysfunction, and Alzheimer's disease. *Mol. Neurodegener.* **14**, 24 (2019).
54. Lunghi, C., Emir, U. E., Morrone, M. C. & Bridge, H. Short-term monocular deprivation alters GABA in the adult human visual cortex. *Curr. Biol.* **25**, 1496–1501 (2015).
55. Loerch, P. M. et al. Evolution of the aging brain transcriptome and synaptic regulation. *PLoS ONE* **3**, e3329 (2008).
56. Stanley, D. P. & Shetty, A. K. Aging in the rat hippocampus is associated with widespread reductions in the number of glutamate decarboxylase-67 positive interneurons but not interneuron degeneration. *J. Neurochem.* **89**, 204–216 (2004).
57. Caspary, D. M., Milbrandt, J. C. & Helfert, R. H. Central auditory aging: GABA changes in the inferior colliculus. *Exp. Gerontol.* **30**, 349–360 (1995).
58. Hua, T., Kao, C., Sun, Q., Li, X. & Zhou, Y. Decreased proportion of GABA neurons accompanies age-related degradation of neuronal function in cat striate cortex. *Brain Res. Bull.* **75**, 119–125 (2008).
59. Stagg, C. J., Bachtari, V. & Johansen-Berg, H. What are we measuring with GABA magnetic resonance spectroscopy? *Commun. Integr. Biol.* **4**, 573–575 (2011).
60. Hendry, S. H., Fuchs, J., deBlas, A. L. & Jones, E. G. Distribution and plasticity of immunocytochemically localized GABAA receptors in adult monkey visual cortex. *J. Neurosci.* **10**, 2438–2450 (1990).
61. Gu, M. et al. GABA editing with macromolecule suppression using an improved MEGA-SPECIAL sequence. *Magn. Reson. Med.* **79**, 41–47 (2018).
62. Wu, G. K., Arbuckle, R., Liu, B. H., Tao, H. W. & Zhang, L. I. Lateral sharpening of cortical frequency tuning by approximately balanced inhibition. *Neuron* **58**, 132–143 (2008).
63. Leventhal, A. G., Wang, Y., Pu, M., Zhou, Y. & Ma, Y. GABA and its agonists improved visual cortical function in senescent monkeys. *Science* **300**, 812–815 (2003).
64. Cook, E., Hammett, S. T. & Larsson, J. GABA predicts visual intelligence. *Neurosci. Lett.* **632**, 50–54 (2016).
65. Stagg, C. J., Bachtari, V. & Johansen-Berg, H. The role of GABA in human motor learning. *Curr. Biol.* **21**, 480–484 (2011).
66. Borojerdi, B., Battaglia, F., Muellbacher, W. & Cohen, L. G. Mechanisms underlying rapid experience-dependent plasticity in the human visual cortex. *Proc. Natl Acad. Sci. USA* **98**, 14698–14701 (2001).
67. Park, S. et al. Shorter sleep duration is associated with lower GABA levels in the anterior cingulate cortex. *Sleep. Med.* **71**, 1–7 (2020).
68. Qiu, M., Ramulu, P. Y. & Boland, M. V. Association between sleep parameters and glaucoma in the United States population: national health and nutrition examination survey. *J. Glaucoma* **28**, 97–104 (2019).
69. Wang, H., Zhang, Y., Ding, J. & Wang, N. Changes in the circadian rhythm in patients with primary glaucoma. *PLoS ONE* **8**, e62841 (2013).
70. Carp, J., Park, J., Polk, T. A. & Park, D. C. Age differences in neural distinctiveness revealed by multi-voxel pattern analysis. *Neuroimage* **56**, 736–743 (2011).
71. Bowman, C. R., Chamberlain, J. D. & Dennis, N. A. Sensory representations supporting memory specificity: age effects on behavioral and neural discriminability. *J. Neurosci.* **39**, 2265–2275 (2019).
72. Dudek, F. E. & Sutula, T. P. Epileptogenesis in the dentate gyrus: a critical perspective. *Prog. Brain Res.* **163**, 755–773 (2007).
73. Atallah, B. V. & Scanziani, M. Instantaneous modulation of gamma oscillation frequency by balancing excitation with inhibition. *Neuron* **62**, 566–577 (2009).
74. Haider, B., Duque, A., Hasenstaub, A. R. & McCormick, D. A. Neocortical network activity in vivo is generated through a dynamic balance of excitation and inhibition. *J. Neurosci.* **26**, 4535–4545 (2006).
75. Mathews, G. C. & Diamond, J. S. Neuronal glutamate uptake contributes to GABA synthesis and inhibitory synaptic strength. *J. Neurosci.* **23**, 2040–2048 (2003).
76. Findley, C. A., Bartke, A., Hascup, K. N. & Hascup, E. R. Amyloid beta-related alterations to glutamate signaling dynamics during Alzheimer's disease progression. *ASN Neuro* **11**, 1759091419855541 (2019).
77. Siskova, Z. et al. Dendritic structural degeneration is functionally linked to cellular hyperexcitability in a mouse model of Alzheimer's disease. *Neuron* **84**, 1023–1033 (2014).
78. Hascup, K. N. & Hascup, E. R. Altered neurotransmission prior to cognitive decline in AbetaPP/PS1 mice, a model of Alzheimer's disease. *J. Alzheimers Dis.* **44**, 771–776 (2015).
79. Minkeviciene, R. et al. Age-related decrease in stimulated glutamate release and vesicular glutamate transporters in APP/PS1 transgenic and wild-type mice. *J. Neurochem.* **105**, 584–594 (2008).
80. Rupsingh, R., Borrie, M., Smith, M., Wells, J. L. & Bartha, R. Reduced hippocampal glutamate in Alzheimer disease. *Neurobiol. Aging* **32**, 802–810 (2011).
81. Kantarci, K. et al. Proton MR spectroscopy in mild cognitive impairment and Alzheimer disease: comparison of 1.5 and 3 T. *AJNR Am. J. Neuroradiol.* **24**, 843–849 (2003).
82. Muthukumaraswamy, S. D., Edden, R. A., Jones, D. K., Swettenham, J. B. & Singh, K. D. Resting GABA concentration predicts peak gamma frequency and fMRI amplitude in response to visual stimulation in humans. *Proc. Natl Acad. Sci. USA* **106**, 8356–8361 (2009).
83. Violante, I. R. et al. GABA deficit in the visual cortex of patients with neurofibromatosis type 1: genotype-phenotype correlations and functional impact. *Brain* **136**, 918–925 (2013).
84. Bridge, H. et al. Altered neurochemical coupling in the occipital cortex in migraine with visual aura. *Cephalalgia* **35**, 1025–1030 (2015).
85. Bednarik, P. et al. Neurochemical and BOLD responses during neuronal activation measured in the human visual cortex at 7 Tesla. *J. Cereb. Blood Flow. Metab.* **35**, 601–610 (2015).
86. Ip, I. B. et al. Combined fMRI-MRS acquires simultaneous glutamate and BOLD-fMRI signals in the human brain. *Neuroimage* **155**, 113–119 (2017).

87. Schallmo, M. P. et al. Glutamatergic facilitation of neural responses in MT enhances motion perception in humans. *Neuroimage* **184**, 925–931 (2019).
88. Kiemes, A. et al. GABA, glutamate and neural activity: a systematic review with meta-analysis of multimodal (1)H-MRS-fMRI studies. *Front. Psychiatry* **12**, 644315 (2021).
89. Donahue, M. J., Near, J., Blicher, J. U. & Jezzard, P. Baseline GABA concentration and fMRI response. *Neuroimage* **53**, 392–398 (2010).
90. Muthukumaraswamy, S. D., Evans, C. J., Edden, R. A., Wise, R. G. & Singh, K. D. Individual variability in the shape and amplitude of the BOLD-HRF correlates with endogenous GABAergic inhibition. *Hum. Brain Mapp.* **33**, 455–465 (2012).
91. Enzi, B. et al. Glutamate modulates resting state activity in the perigenual anterior cingulate cortex - a combined fMRI-MRS study. *Neuroscience* **227**, 102–109 (2012).
92. Duncan, N. W. et al. Negative childhood experiences alter a prefrontal-insular-motor cortical network in healthy adults: A preliminary multimodal rsfMRI-fMRI-MRS-dMRI study. *Hum. Brain Mapp.* **36**, 4622–4637 (2015).
93. Duncan, N. W., Enzi, B., Wiebking, C. & Northoff, G. Involvement of glutamate in rest-stimulus interaction between perigenual and supragenual anterior cingulate cortex: a combined fMRI-MRS study. *Hum. Brain Mapp.* **32**, 2172–2182 (2011).
94. Cadena, E. J. et al. A longitudinal multimodal neuroimaging study to examine relationships between resting state glutamate and task related BOLD response in schizophrenia. *Front Psychiatry* **9**, 632 (2018).
95. Dreyer, E. B., Zurakowski, D., Schumer, R. A., Podos, S. M. & Lipton, S. A. Elevated glutamate levels in the vitreous body of humans and monkeys with glaucoma. *Arch. Ophthalmol.* **114**, 299–305 (1996).
96. Brooks, D. E., Garcia, G. A., Dreyer, E. B., Zurakowski, D. & Franco-Bourland, R. E. Vitreous body glutamate concentration in dogs with glaucoma. *Am. J. Vet. Res.* **58**, 864–867 (1997).
97. Carter-Dawson, L. et al. Vitreal glutamate concentration in monkeys with experimental glaucoma. *Invest. Ophthalmol. Vis. Sci.* **43**, 2633–2637 (2002).
98. Honkanen, R. A. et al. Vitreous amino acid concentrations in patients with glaucoma undergoing vitrectomy. *Arch. Ophthalmol.* **121**, 183–188 (2003).
99. Gramlich, O. W., Godwin, C. R., Wadkins, D., Elwood, B. W. & Kuehn, M. H. Early functional impairment in experimental glaucoma is accompanied by disruption of the GABAergic system and inceptive neuroinflammation. *Int. J. Mol. Sci.* **22**, 7581 (2021).
100. Zhou, X., Zhang, R., Zhang, S., Wu, J. & Sun, X. Activation of 5-HT1A receptors promotes retinal ganglion cell function by inhibiting the cAMP-PKA pathway to modulate presynaptic GABA release in chronic glaucoma. *J. Neurosci.* **39**, 1484–1504 (2019).
101. Zhou, X. et al. Alpha7 nicotinic acetylcholine receptor agonist promotes retinal ganglion cell function via modulating GABAergic presynaptic activity in a chronic glaucomatous model. *Sci. Rep.* **7**, 1734 (2017).
102. Cello, K. E., Nelson-Quigg, J. M. & Johnson, C. A. Frequency doubling technology perimetry for detection of glaucomatous visual field loss. *Am. J. Ophthalmol.* **129**, 314–322 (2000).
103. Burgansky-Eliash, Z. et al. Optical coherence tomography machine learning classifiers for glaucoma detection: a preliminary study. *Invest. Ophthalmol. Vis. Sci.* **46**, 4147–4152 (2005).
104. Mohammadzadeh, V. et al. Longitudinal macular structure-function relationships in glaucoma. *Ophthalmology* **127**, 888–900 (2020).
105. Nouri-Mahdavi, K. et al. Prediction of visual field progression from OCT structural measures in moderate to advanced glaucoma. *Am. J. Ophthalmol.* **226**, 172–181 (2021).
106. Provencher, S. W. Automatic quantitation of localized in vivo 1H spectra with LCModel. *NMR Biomed.* **14**, 260–264 (2001).
107. Provencher, S. W. Estimation of metabolite concentrations from localized in vivo proton NMR spectra. *Magn. Reson. Med.* **30**, 672–679 (1993).
108. Trivedi, V. et al. Widespread brain reorganization perturbs visuomotor coordination in early glaucoma. *Sci. Rep.* **9**, 14168 (2019).
109. Brainard, D. H. The psychophysics toolbox. *Spat. Vis.* **10**, 433–436 (1997).
110. Bang, J. W. Data sets for GABA reduction in the visual cortex of glaucoma patients. OSF <https://doi.org/10.17605/OSF.IO/85CDS> (2022)

Acknowledgements

The authors would like to thank Ms Tonya Robins, Zena Moore, Jamika Singleton-Garvin and members of the Neuroimaging and Visual Science Laboratory at New York University Grossman School of Medicine for their help with subject recruitment and technical support. This work is supported in part by the National Institutes of Health R01-EY028125, R01-EY013178, and P41-EB017183 (Bethesda, Maryland), BrightFocus Foundation G2016030, G2019103, and G2021001F (Clarksburg, Maryland), and an unrestricted grant from Research to Prevent Blindness to NYU Langone Health Department of Ophthalmology (New York, NY).

Author contributions

J.W.B., C.P., G.W., J.S.S., and K.C.C. conceived and designed experiments. J.W.B. and C.P. carried out experiments. J.W.B., C.P., and K.Y. analyzed the data. G.W., J.S.S., and K.C.C. supervised the experiments. J.W.B., C.P., K.Y., G.W., J.S.S., and K.C.C. wrote the article.

Competing interests

J.S.S. declares the following competing interests: Royalties e Zeiss, Dublin, CA.

Additional information


Supplementary information The online version contains supplementary material available at <https://doi.org/10.1038/s42003-023-04918-8>.

Correspondence and requests for materials should be addressed to Ji Won Bang or Kevin C. Chan.

Peer review information *Communications Biology* thanks Molly Simmonite and Jihong Wu for their contribution to the peer review of this work. Primary Handling Editors: Joao Valente.

Reprints and permission information is available at <http://www.nature.com/reprints>

Publisher's note Springer Nature remains neutral with regard to jurisdictional claims in published maps and institutional affiliations.

 **Open Access** This article is licensed under a Creative Commons Attribution 4.0 International License, which permits use, sharing, adaptation, distribution and reproduction in any medium or format, as long as you give appropriate credit to the original author(s) and the source, provide a link to the Creative Commons license, and indicate if changes were made. The images or other third party material in this article are included in the article's Creative Commons license, unless indicated otherwise in a credit line to the material. If material is not included in the article's Creative Commons license and your intended use is not permitted by statutory regulation or exceeds the permitted use, you will need to obtain permission directly from the copyright holder. To view a copy of this license, visit <http://creativecommons.org/licenses/by/4.0/>.

© The Author(s) 2023